DOI: 10.13009/EUCASS2019-713

Using Differential Flatness for solving the Minimum-Fuel Low-Thrust Geostationary Station-Keeping Problem

C. Gazzino[†], *C. Louembet*[⋆]

[⋆]*CNRS, LAAS-CNRS, Université de Toulouse*
7 avenue du Colonel Roche, 31031 Toulouse cedex 4, France

clement.gazzino@isae-alumni.net · clouembe@laas.fr
[†]Corresponding author

Abstract

The minimum fuel station keeping of a geostationary satellite equipped with electric thrusters undergoing the Earth non-spherical disturbing gravitational potential up to degree and order 2 is first recast by transforming the linear time varying relative dynamics in a time invariant one with a Floquet-Lyapunov transformation. In a second step, the flatness property of the system is used to convert the genuine optimal control problem to a linear programming problem. This problem is solved for an ideal geostationary satellite with one thruster mounted on each face.

1. Introduction

Spacecraft orbiting the Earth on Geostationary Earth Orbits (GEO) undergo orbital disturbing forces, resulting in a natural drift. This drift pushes the spacecraft outside their operational station keeping (SK) windows (a rectangular box of a given geographical longitude and latitude range). It is therefore mandatory to design an accurate SK guidance strategy, in order not to let the spacecraft operating conditions deteriorate.

The usual spacecraft propulsion system is composed of chemical thrusters (see Soop[32] or Sidi[30]). However, the idea of using electric propulsion has been proposed in the sixties (see for instance Barret[3] or Hunziker[17]), followed by some theoretical developments in the eighties (as for example the development conducted by Anzel[2]). This kind of propulsion system is a viable alternative to the commonly used chemical one thanks to its high specific impulse. Indeed, this particular feature naturally imply fuel consumption savings enabling to increase the spacecraft longevity, and has been successfuly used for the Eurostar 3000 platform (see Demairé[8]).

A whole venue of works addresses the resolution of constrained optimal control problem. These works have been classified in two families: the direct and indirect methods (see Betts[5] or Hull[16] for details on this classification). The indirect methods rely on the necessary optimality conditions of the Pontryagin Maximum Principle (PMP) and the resolution of the Two-point-boundary-value problem. The direct methods aim to transcribe the OCP into a constrained optimization program, the optimality conditions being ensured by the Karush-Kuhn-Tucker conditions. To obtain such a program, different techniques are available, the most popular being the discretisation-based collocation method where both dynamics and constraints are satisfied discretely.

An alternative direct method for solving OCP is based on the notion of differential flatness. This notion relates to a dynamic feedback of the system, see for instance Fliess[10–12] or more recently Lévine.[19] Roughly speaking, a controllable system admits flat outputs so that any state and input histories can be computed from these flat outputs (and its derivatives) without integration. Moreover, these new variables undergo a trivial dynamics, and consequently they are differentially independent from each others. As a consequence, the OCP expressed in terms of the system flat outputs is differential-constraint free since this constraint is trivially satisfied. Then, with a suitable parametrization of these flat outputs, the original OCP is recast to a nonlinear programming problem. In the case where the original dynamics is linear time invariant, algorithm exists for the computation of the flat outputs, see Sontag,[31] Lévine[20] or Ford[14] for instance.

Differential flatness has been applied for several kinds of systems. For instance, the reference Murray[26] exhibits the flat outputs for a wide range of mechanical systems. For spacecraft control, Louembet[22] applies the differential

DOI: 10.13009/EUCASS2019-713

flatness theory for attitude slew manoeuvres computation. For spacecraft trajectory optimisation, the work of Louembet[23] solves a collision avoidance low-thrust rendez-vous with splines based parametrization of the flat outputs and the recent work of Farahani[9] solves the path planning problem for autonomous docking. Regarding geostationary station keeping, the reference Losa[21] uses differential flatness in the case of simplified dynamic matrix with only two non-zero terms. In this paper, the GEO dynamics is enhanced to account for the disturbing part of the Earth potential up to degree and order 2. The novelty of the proposed paper is to compute the flat outputs for the considered time varying model. Our contribution consists in adapting existing algorithms for computing flat outputs and thus obtaining time varying flat outputs transformations (see for instance Sontag[31]). After a parametrization by splines functions, the genuine SK optimal control is transformed into a linear programming problem. An illustration of the results is performed using an ideal GEO spacecraft with one thruster mounted on each face.

2. Geostationary Station-Keeping Problem

2.1 Geostationary Spacecraft Dynamics

The motion of a spacecraft orbiting the Earth on a GEO can be described with the equinoctial orbital elements as defined in Battin:[4]

$$x_{eoe} = \begin{bmatrix} a & e_x & e_y & i_x & i_y & \ell_{M\Theta} \end{bmatrix}^T, \tag{1}$$

where a is the semi-major axis, $(e_x,\ e_y)$ the eccentricity vector, (i_x, i_y) the inclination vector, $\ell_{M\Theta} = \omega + \Omega + M - \Theta(t)$ is the mean longitude where Ω is the right ascension of the ascending node, ω is the perigee's argument, M is the mean anomaly and $\Theta(t)$ is the right ascension of the Greenwich meridian.

The non-linear dynamics of the GEO satellite is given by:

$$\frac{dx_{eoe}}{dt} = K(x_{eoe}) + L(x_{eoe})\frac{\partial V_{\text{dist}}(x_{eoe})}{\partial x_{eoe}} + G(x_{eoe})v, \tag{2}$$

where $K(x_{eoe})$ is the Keplerian part of the dynamics, $L(x_{eoe})$ the Lagrangian matrix, V_{dist} the disturbing potential, $G(x_{eoe})$ the Gauss matrix and v the disturbing external force. In such a description, the disturbing potential and the disturbing force are assumed to be small relatively to the Keplerian attraction. The expression of $K(x_{eoe})$, $L(x_{eoe})$ and $G(x_{eoe})$ can be found in Losa.[21]

Spacecraft orbiting the Earth on a GEO orbit undergo three main orbital disturbances: the non-spherical Earth gravitational potential, the lunisolar attraction from the Sun and the Moon, and the Sun radiation pressure. This study focusses solely on the effects of Earth disturbing gravitationnal potential up to the degree and order 2. These disturbing terms expressed by means of the equinoctial orbital elements are given in Appendix A.

The satellite is equipped with an ideal electric propulsion system with a thruster mounted on each face. The control acceleration created by these thrusters $v = \begin{bmatrix} v_R & v_T & v_N \end{bmatrix}^T$ is expressed in the local orbital RTN frame (also written RSW) and defined by Soop[32] as N being the unit vector along the kinetic momentum, R being the unit vector in the direction Earth's center - satellite and T completing the right-handed orthogonal basis.

The satellite has to remain near its Station Keeping (SK) state:

$$x_{sk} = \begin{bmatrix} a_{sk} & 0 & 0 & 0 & 0 & \ell_{M\Theta,sk} \end{bmatrix}^T, \tag{3}$$

with a_{sk} the SK semi-major axis (see Appendix C) and $\ell_{M\Theta,sk}$ the mean longitude. Therefore, the non linear equation of motion (2) can be linearized around this nominal state. Defining the relative SK state as:

$$x = \begin{bmatrix} \frac{a-a_{sk}}{a_{sk}} & e_x & e_y & i_x & i_y & \ell_{M\Theta} - \ell_{M\Theta,sk} \end{bmatrix}, \tag{4}$$

the linearized dynamics reads:

$$\frac{dx}{dt} = A(t)x + D(t) + \sqrt{\frac{\mu}{a_{sk}}}B(t)v, \tag{5}$$

with the expressions of the matrices A, B and D given in Appendix B.

For convenience, the control vector v is transformed to:

$$u = \sqrt{\frac{\mu}{a_{sk}}}v. \tag{6}$$

The nonlinear dynamics equation (5) is rewritten as:

$$\frac{dx}{dt} = A(t)x + D(t) + B(t)u. \tag{7}$$

DOI: 10.13009/EUCASS2019-713

2.2 Floquet-Lyapunov Transformation of the Dynamics

As the dynamics matrix of the Linear Time Varying (LTV) system given by Equation (5) is periodic, it is possible to apply the Floquet-Lyapinov theory as in Brentari,[6] Deaconnu[7] and Sherill[29] so as to look for a periodic similarity transformation in order to transform the system (7) into a Linear Time Invariant (LTI) one.

Denoting $t \mapsto W(t)$ the Floquet-Lyapunov transformation, and ζ the new state vector such that $\zeta = W(t)x$, the new dynamics is expressed as:

$$
\begin{aligned}
\dot{\zeta}(t) &= (\dot{W}(t)W^{-1}(t) + W(t)A(t)W^{-1}(t))\zeta(t) + W(t)D(t) + W(t)B(t)u(t),\\
&= \tilde{A}\zeta(t) + \tilde{D} + \tilde{B}u(t),
\end{aligned}
\tag{8}
$$

where matrices $\tilde{A}$, $\tilde{B}$ and $\tilde{D}$ are time invariant.

In the context of the relative dynamics of a GEO spacecraft, the proposed transformation is adapted from the one given by Losa:[21]

$$
W(t) = \begin{bmatrix} 0 & -S_\kappa & C_\kappa & 0 & 0 & -\frac{1}{2} \\ 0 & -S_\kappa & C_\kappa & 0 & 0 & -\frac{3}{4} \\ -1 & C_\kappa & S_\kappa & 0 & 0 & 0 \\ 0 & 0 & 0 & -S_\kappa & C_\kappa & 0 \\ 0 & 0 & 0 & C_\kappa & S_\kappa & 0 \\ -1 & S_\kappa & -C_\kappa & 0 & 0 & 0 \end{bmatrix},
\tag{9}
$$

with $C_\kappa = \cos\kappa_{sk}(t)$, $S_\kappa = \sin\kappa_{sk}(t)$ and $\kappa_{sk}(t) = \ell_{M\Theta} + \Theta(t)$.

The matrix $W(t)$ is bounded and non singular for every t with a determinant W(t) $= \frac{1}{4} \neq 0$. The inverse of the transformation is given by:

$$
W^{-1}(t) = \begin{bmatrix} -3 & 2 & 0 & 0 & 0 & -1 \\ -3(C_\kappa + S_\kappa) & 2(C_\kappa + S_\kappa) & C_\kappa & 0 & 0 & -C_\kappa \\ 3(C_\kappa - S_\kappa) & 2(-C_\kappa + S_\kappa) & S_\kappa & 0 & 0 & -S_\kappa \\ 0 & 0 & 0 & -S_\kappa & C_\kappa & 0 \\ 0 & 0 & 0 & C_\kappa & S_\kappa & 0 \\ 4 & -4 & 0 & 0 & 0 & 0 \end{bmatrix},
\tag{10}
$$

and its derivative is:

$$
\dot{W} = \omega_e \begin{bmatrix} 0 & -C_\kappa & -S_\kappa & 0 & 0 & 0 \\ 0 & -C_\kappa & -S_\kappa & 0 & 0 & 0 \\ 0 & -S_\kappa & C_\kappa & 0 & 0 & 0 \\ 0 & 0 & 0 & -C_\kappa & -S_\kappa & 0 \\ 0 & 0 & 0 & -S_\kappa & C_\kappa & 0 \\ 0 & C_\kappa & S_\kappa & 0 & 0 & 0 \end{bmatrix},
\tag{11}
$$

with ω_e the Earth mean rotation rate, whose value is given in Appendix C.

With the proposed Floquet-Lyapunov transformation, the new dynamics matrices $\tilde{A}$, $\tilde{D}$ and $\tilde{C}$ are explicitely defined by:

$$
\begin{cases}
\tilde{A} = \dot{W}(t)W^{-1}(t) + \tilde{A}_K + \tilde{A}_{C_{20}} + \tilde{A}_{C_{21}} + \tilde{A}_{S_{21}} + \tilde{A}_{C_{22}} + \tilde{A}_{S_{22}},\\
\tilde{D} = \tilde{D}_K + \tilde{D}_{C_{20}} + \tilde{D}_{C_{21}} + \tilde{D}_{S_{21}} + \tilde{D}_{C_{22}} + \tilde{D}_{S_{22}},
\end{cases}
\tag{12}
$$

with :

$$
\dot{W}(t)W^{-1}(t) = \omega_e \begin{bmatrix} 3 & -2 & -1 & 0 & 0 & 1 \\ 3 & -2 & -1 & 0 & 0 & 1 \\ 3 & -2 & 0 & 0 & 0 & 0 \\ 0 & 0 & 0 & 0 & -1 & 0 \\ 0 & 0 & 0 & 1 & 0 & 0 \\ -3 & 2 & 1 & 0 & 0 & -1 \end{bmatrix},
\tag{13}
$$

$$
\tilde{A}_K = WA_KW^{-1} = \gamma_K \begin{bmatrix} -\frac{3}{2} & -1 & 0 & 0 & 0 & \frac{1}{2} \\ \frac{9}{4} & -\frac{3}{2} & 0 & 0 & 0 & \frac{3}{4} \\ 0 & 0 & 0 & 0 & 0 & 0 \\ 0 & 0 & 0 & 0 & 0 & 0 \\ 0 & 0 & 0 & 0 & 0 & 0 \\ 0 & 0 & 0 & 0 & 0 & 0 \end{bmatrix},
\tag{14}
$$

DOI: 10.13009/EUCASS2019-713

$$\tilde{A}_{C_{20}} = WA_{C_{20}}W^{-1} = \alpha_{20}\begin{bmatrix} -\frac{3}{8} & \frac{1}{4} & \frac{29}{8} & 0 & 0 & -\frac{1}{8} \\ -\frac{3}{16} & \frac{1}{8} & \frac{71}{16} & 0 & 0 & -\frac{1}{16} \\ 4 & -2 & 0 & 0 & 0 & 0 \\ 0 & 0 & 0 & 0 & 0 & 0 \\ 0 & 0 & 0 & 1 & 0 & 0 \\ \frac{15}{4} & -\frac{5}{2} & -2 & 0 & 0 & \frac{1}{4} \end{bmatrix}, \tag{15}$$

$$\tilde{A}_{C_{21}} = WA_{C_{21}}W^{-1} = \alpha_{21}\begin{bmatrix} 0 & 0 & 0 & \frac{13}{2}C_\ell & 0 & 0 \\ 0 & 0 & 0 & \frac{57}{4}C_\ell & 0 & 0 \\ 0 & 0 & 0 & -4S_\ell & 4C_\ell & 0 \\ -2C_\ell & 2C_\ell & 0 & 0 & 0 & 0 \\ -\frac{3}{4}C_\ell + 2S_\ell & \frac{1}{2}C_\ell - 2S_\ell & -\frac{3}{2}C_\ell & 0 & 0 & -\frac{1}{4}C_\ell \\ 0 & 0 & 0 & -6C_\ell - 4S_\ell & -4C_\ell & 0 \end{bmatrix}, \tag{16}$$

$$\tilde{A}_{S_{21}} = WA_{S_{21}}W^{-1} = \beta_{21}\begin{bmatrix} 0 & 0 & 0 & \frac{1}{2}S_\ell & 0 & 0 \\ 0 & 0 & 0 & -\frac{9}{4}S_\ell & 0 & 0 \\ 0 & 0 & 0 & 4C_\ell & -4S_\ell & 0 \\ -2S_\ell & 2S_\ell & 0 & 0 & 0 & 0 \\ -2C_\ell - \frac{3}{4}S_\ell & 2C_\ell + \frac{1}{2}S_\ell & -\frac{3}{2}S_\ell & 0 & 0 & -\frac{1}{4}C_\ell \\ 0 & 0 & 0 & -6C_\ell - 4S_\ell & -4C_\ell & 0 \end{bmatrix}, \tag{17}$$

$$\tilde{A}_{C_{22}} = WA_{C_{22}}W^{-1} = \alpha_{22}\begin{bmatrix} -\frac{9}{4}C_{2\ell} - 23S_{2\ell} & \frac{3}{2}C_{2\ell} - 6S_{2\ell} & -\frac{81}{4}C_{2\ell} & 0 & 0 & -\frac{3}{4}C_{2\ell} \\ -\frac{45}{8}C_{2\ell} - \frac{55}{2}C_{2\ell} & \frac{15}{4}C_{2\ell} - 7S_{2\ell} & -\frac{195}{8}C_{2\ell} & 0 & 0 - \frac{15}{8}C_{2\ell} & \\ -56C_{2\ell} - 36S_{2\ell} & 12C_{2\ell} + 24S_{2\ell} & 36S_{2\ell} & 0 & 0 & -12S_{2\ell} \\ 0 & 0 & 0 & 0 & 2S_{2\ell} & 0 \\ 0 & 0 & 0 & -2C_{2\ell} & 2S_{2\ell} & 0 \\ -\frac{77}{2}C_{2\ell} - 16S_{2\ell} & 15C_{2\ell} + 24S_{2\ell} & 12C_{2\ell} + 20S_{2\ell} & 0 & 0 & -\frac{3}{2}C_{2\ell} - 10S_{2\ell} \end{bmatrix}, \tag{18}$$

$$\tilde{A}_{S_{22}} = WA_{S_{22}}W^{-1} = \beta_{22}\begin{bmatrix} -\frac{9}{4}S_{2\ell} + 23C_{2\ell} & \frac{3}{2}S_{2\ell} + 6C_{2\ell} & -\frac{81}{4}S_{2\ell} & 0 & 0 & -\frac{3}{4}S_{2\ell} \\ -\frac{45}{8}S_{2\ell} + \frac{55}{2}C_{2\ell} & \frac{15}{4}S_{2\ell} + 7C_{2\ell} & -\frac{195}{8}S_{2\ell} & 0 & 0 - \frac{15}{8}S_{2\ell} & \\ 36C_{2\ell} - \frac{45}{8}S_{2\ell} & 12S_{2\ell} - 24C_{2\ell} & -36C_{2\ell} & 0 & 0 & 12C_{2\ell} \\ 0 & 0 & 0 & 0 & 0 & 0 \\ 0 & 0 & 0 & -2S_{2\ell} & 2C_{2\ell} & 0 \\ -\frac{77}{2}S_{2\ell} + 16C_{2\ell} & 15S_{2\ell} - 24C_{2\ell} & 12S_{2\ell} - 20C_{2\ell} & 0 & 0 & -\frac{3}{2}S_{2\ell} + 10C_{2\ell} \end{bmatrix}, \tag{19}$$

$$\tilde{D}_K = WD_K = \delta_K\begin{bmatrix} -\frac{1}{2} & -\frac{3}{4} & 0 & 0 & 0 & 0 \end{bmatrix}^T, \tag{20}$$

$$\tilde{D}_{C_{20}} = WD_{C_{20}} = \alpha_{20}\begin{bmatrix} 1 & \frac{5}{4} & 0 & 0 & 0 & -\frac{1}{2} \end{bmatrix}^T, \tag{21}$$

$$\tilde{D}_{C_{21}} = WD_{C_{21}} = \alpha_{21}\begin{bmatrix} 0 & 0 & 0 & 0 & \frac{1}{2}C_\ell & 0 \end{bmatrix}^T, \tag{22}$$

$$\tilde{D}_{S_{21}} = WD_{S_{21}} = \beta_{21}\begin{bmatrix} 0 & 0 & 0 & 0 & -\frac{1}{2}S_\ell & 0 \end{bmatrix}^T, \tag{23}$$

$$\tilde{D}_{C_{22}} = WD_{C_{22}} = \alpha_{22}\begin{bmatrix} -6C_{2\ell} & -\frac{15}{2}C_{2\ell} & 8S_{2\ell} & 0 & 0 & 3C_{2\ell} + 4S_{2\ell} \end{bmatrix}^T, \tag{24}$$

$$\tilde{D}_{S_{22}} = WD_{S_{22}} = \beta_{22}\begin{bmatrix} -6S_{2\ell} & -\frac{15}{2}S_{2\ell} & -8C_{2\ell} & 0 & 0 & 3S_{2\ell} - 4C_{2\ell} \end{bmatrix}^T, \tag{25}$$

DOI: 10.13009/EUCASS2019-713

$$\tilde{B} = WB = \begin{bmatrix} 0 & 0 & 0 \\ \frac{1}{2} & 0 & 0 \\ 0 & 0 & 0 \\ 0 & 0 & 0 \\ 0 & 0 & \frac{1}{2} \\ 1 & -2 & 0 \end{bmatrix}, \tag{26}$$

Putting together the matrices given by Equations (14)-(25) and symplifying trigonometric expressions lead to the new dynamics system defined by:

$$\tilde{A} = \begin{bmatrix} -\frac{9}{4}\eta_{C_{22}} + \frac{92}{4}\eta_{S_{22}} + \frac{3}{2}\gamma_K + \frac{3}{8}\alpha_{20} + 3\omega_e & \frac{3}{2}\eta_{C_{22}} + 6\eta_{S_{22}} - \gamma_K - \frac{1}{4}\alpha_{20} - 2\omega_e & -\frac{81}{4}\eta_{C_{22}} + \frac{29}{8}\alpha_{20} - \omega_e & 11C_\ell\alpha_{21} + \frac{1}{2}\eta_{C_{21}} & 0 & -\frac{3}{4}\eta_{C_{22}} + \frac{1}{2}\gamma_K - \frac{1}{8}\alpha_{20} + \omega_e \\ -\frac{45}{8}\eta_{C_{22}} + \frac{55}{2}\eta_{S_{22}} + \frac{9}{4}\gamma_K - \frac{3}{16}\alpha_{20} + 3\omega_e & \frac{15}{4}\eta_{C_{22}} + \frac{28}{4}\eta_{S_{22}} - \frac{3}{2}\gamma_K + \frac{1}{8}\alpha_{20} - 2\omega_e & -\frac{195}{8}\eta_{C_{22}} + \frac{71}{16}\alpha_{20} - \omega_e & -\frac{9}{4}\eta_{C_{21}} + \frac{33}{2}C_\ell\alpha_{21} & 0 & -\frac{15}{8}\eta_{C_{22}} + \frac{3}{4}\gamma_K - \frac{1}{16}\alpha_{20} + \omega_e \\ -56\eta_{C_{22}} + 36\eta_{S_{22}} + 4\alpha_{20} + 3\omega_e & 12\eta_{C_{22}} - 24\eta_{S_{22}} - 2\alpha_{20} - 2\omega_e & -36\eta_{S_{22}} & 4\eta_{S_{21}} & -4\eta_{C_{21}} & 12\eta_{S_{22}} \\ -2\eta_{C_{21}} & 2\eta_{C_{21}} & 0 & 0 & -\omega_e & 0 \\ -\frac{3}{4}\eta_{C_{22}} - 2\eta_{S_{22}} & \frac{1}{2}\eta_{C_{22}} + 2\eta_{S_{22}} & -\frac{3}{2}\eta_{C_{22}} & -2\eta_{C_{22}} + \alpha_{20} + \omega_e & 2\eta_{S_{22}} & -\frac{1}{4}\eta_{C_{21}} \\ \frac{77}{2}\eta_{C_{22}} + 16\eta_{S_{22}} + \frac{15}{4}\alpha_{20} - 3\omega_e & 15\eta_{C_{22}} - 24\eta_{S_{22}} - \frac{5}{2}\alpha_{20} + 2\omega_e & 12\eta_{C_{22}} - 20\eta_{S_{22}} - 2\alpha_{20} + \omega_e & -6\eta_{C_{21}} + 4\eta_{S_{21}} & -4\eta_{C_{21}} & -\frac{3}{2}\eta_{C_{22}} + 10\eta_{S_{22}} + \frac{1}{4}\alpha_{20} - \omega_e \end{bmatrix}, \tag{27a}$$

$$\tilde{D} = \begin{bmatrix} \frac{1}{2}\delta_K + \alpha_{20} - 6\eta_{C_{22}} \\ -\frac{3}{4}\delta_K + \frac{5}{4}\alpha_{20} - \frac{15}{2}\eta_{C_{22}} \\ -8\eta_{S_{22}} \\ 0 \\ \frac{1}{2}\bar{\eta}_{C_{21}} \\ -\frac{1}{2}\alpha_{20} + 3\eta_{C_{22}} - 4\eta_{S_{22}} \end{bmatrix}, \tag{27b}$$

with:

$$\begin{cases} \eta_{C_{21}} = \alpha_{21}C_\ell + \beta_{21}S_\ell, \\ \bar{\eta}_{C_{21}} = \alpha_{21}C_\ell - \beta_{21}S_\ell, \\ \eta_{S_{21}} = \beta_{21}C_\ell - \alpha_{21}S_\ell, \\ \eta_{C_{22}} = \alpha_{22}C_{2\ell} + \beta_{22}S_{2\ell}, \\ \eta_{S_{22}} = \beta_{22}C_{2\ell} - \alpha_{22}S_{2\ell}. \end{cases} \tag{28}$$

The constants γ_K, δ_K, α_{20}, α_{21}, β_{21}, α_{22}, β_{22}, C_ℓ, S_ℓ, $C_{2\ell}$ and $S_{2\ell}$ are defined in Appendix B.

As stated in Losa,[21] the transformation given by Equation (9) has been built in order to make the control matrix $B(t)$ time invariant. The novelty of our approach is to consider as dynamic matrix $A(t)$ the true expression of the Earth disturbing potential, and not the simplified one used by Losa[21] for which only the $(6, 1)$ and $(1, 6)$ terms are non-zero.

As the new dynamical system defined by the Equation (8) is LTI, it is possible to compute its state transition matrix as defined by Antsaklis.[1] This matrix is the matrix $\Phi(t, t_0)$ such that:

$$\frac{d\Phi(t, t_0)}{dt} = \tilde{A}(t)\Phi(t, t_0) \text{ and } \Phi(t_0, t_0) = I_6, \tag{29}$$

with I_6 the identity matrix of dimension 6. The state vector $\zeta(t)$ is thus given by:

$$\zeta(t) = e^{\tilde{A}(t-t_0)}\zeta(t_0), \tag{30}$$

and converting back to the relative equinoxial elements thanks to the Floquet-Lyapunov transformation leads to:

$$x(t) = W^{-1}(t)e^{\tilde{A}(t-t_0)}W(t_0)x(t_0). \tag{31}$$

DOI: 10.13009/EUCASS2019-713

2.3 Fuel Optimal Geostationary Station-Keeping Problem

The geographical coordinates of the satellite:

$$y_{eoe} = T(x_{eoe}, t)x_{eoe}, \tag{32}$$

have to be computed as the SK strategy consists in finding the control for maintaining the satellite in the vicinity of the SK position $y_{sk} = \begin{bmatrix} r_{sk} & 0 & \lambda_{sk} \end{bmatrix}^T$, where r_{sk} is the synchronous radius and λ_{sk} is the station keeping geographical longitude. Equation (32) can be linearized about y_{sk}, which leads to the following relative geographical coordinates:

$$y = y_{eoe} - y_{sk} = T(x_{sk}, t)x = C(t)x, \tag{33}$$

with the expression of $C(t)$ being given in Appendix B.

Thanks to the expression of the relative geographical position given by Equation (33) and the proposed Floquet-Lyapunov transformation presented in Section 2.2, the SK requirement of maintaining the satellite in its SK window is given by the following constraints:

$$\begin{cases} \left|\begin{bmatrix} 0 & 1 & 0 \end{bmatrix} C(t)W^{-1}(t)\zeta(t)\right| \leqslant \delta, \\ \left|\begin{bmatrix} 0 & 0 & 1 \end{bmatrix} C(t)W^{-1}(t)\zeta(t)\right| \leqslant \delta, \end{cases} \quad \forall t \in [t_0, t_1], \tag{34}$$

where δ is the half-width of the SK window and $[t_0, t_1]$ the horizon on which the SK problem has to be solved. These constraints are summarized as:

$$\left|C_{\varphi\lambda}(t)W^{-1}(t)\zeta(t)\right| \leqslant \delta_2, \text{ with } C_{\varphi\lambda}(t) = \begin{bmatrix} 0 & 1 & 0 \\ 0 & 0 & 1 \end{bmatrix} \text{ and } \delta_2 = \begin{bmatrix} \delta \\ \delta \end{bmatrix}. \tag{35}$$

As the propulsion system is a low thrust one, the force created by the thrusters is bounded by F_{max}. The control vector $\bar{u}$ must fulfill the following constraint:

$$\forall t \in [t_0, t_1], \; |u_i(t)| \leqslant \sqrt{\frac{\mu}{a_{sk}}} \frac{F_{max}}{m} = U_{\max}, \qquad \text{with } i = R, T, N, \tag{36}$$

with m the satellite mass.

Designing a miniminum fuel SK strategy requires to define the following performance index:

$$J(u) = \int_{t_0}^{t_1} |u(t)|dt \tag{37}$$

The minimum fuel optimal SK problem reads thus:

Problem 1

$$\min_u J(u)$$
$$s.t. \begin{cases} \dot{\zeta}(t) = \tilde{A}\zeta(t) + \tilde{D} + \tilde{B}u(t), \\ \zeta(t_0) \text{ fixed}, \\ \zeta(t_1) \text{ free}, \\ \forall t \in [t_0, t_1], \; \left|C_{\varphi\lambda}(t)W^{-1}(t)\zeta(t)\right| \leqslant \delta_2, \\ \forall t \in [t_0, t_1], \; |u_i(t)| \leqslant U_{\max}, \; i = R, T, N. \end{cases} \tag{38}$$

∘

3. Solving the Optimal Control Problem using Differential Flatness

The previous section introduces the optimal control problem that formalizes the station keeping problem on a fixed time horizon. A methodology is proposed here to solve problem (1) based on the flatness property of the dynamical model (8).

DOI: 10.13009/EUCASS2019-713

3.1 Differential Flatness

The differential flatness theory has been introduced by M. Fliess and co-workers at the beginning of the nineties (see Fliess[12, 13]). This theory has been succesfully applied for solving the optimal control problem once the dynamic system shows the flatness property (see Martin[24]).

Let us consider a very general finite dimensional non linear system of the form:

$$\dot{x}(t) = f(x(t), u(t)), \tag{39}$$

where f is a sufficiently smooth vector field, $u \in \mathbb{R}^m$ is the control vector, $x \in \mathbb{R}^n$ is the state vector.

Definition 1 (Differentially flat system) *System (39) is said to be a flat system if there exists a vector $z \in \mathbb{R}^m$:*

$$z = h(x, u, \dot{u}, \dots, u^{(r)})$$

such that the state vector x and the control vector u can be parametrized as:

$$x = \phi(z, \dot{z}, \dots, z^{(q)}),$$

$$u = \psi(z, \dot{z}, \dots, z^{(q+1)}),$$

where h, ϕ and ψ are smooth vector fields, and r and q are integers.

The variable y is called a flat output for the system (39) (also called linearizing output) and is of dimension m, exactly the numbers of inputs. Notice that according to the definition of a flat system, the state x and the control u should satisfy the differential equation $\dot{x}(t) = f(x(t), u(t))$ and therefore, one have also the following relationship:

$$\dot{\phi}(t) = f(\phi(t), \psi(t)).$$

3.2 Flat Output Computation

In Fliess,[12] it has been shown that the controllability of a linear model is equivalent to its flatness property and ensures the existence of flat outputs. The results state the flat outputs are the Brunovskii output of a any given controllable linear time invariant system,

$$\dot{x} = Ax(t) + Bu(t). \tag{40}$$

The Brunovskii canonical form of a controllable linear system takes the form of a block diagonal controllable system:

$$\dot{\bar{x}}(t) = \bar{A}\bar{x} + \bar{B}\bar{u}(t). \tag{41}$$

Matrices $(\bar{A}, \bar{B})$ are given by:

$$\begin{aligned} \bar{A} &= \mathrm{diag}(\Delta_1, \dots, \Delta_\nu), \\ \bar{B} &= \begin{bmatrix} b_1 & 0 & \dots & 0 & 0\dots & 0 \\ 0 & b_2 & \dots & 0 & 0\dots & 0 \\ \vdots & \vdots & \ddots & \vdots & \ddots & \vdots \\ 0 & 0 \ddots & b_\nu & 0 & \dots & 0 \end{bmatrix}, \end{aligned} \tag{42}$$

where $\Delta_i \in \mathbb{R}^{\kappa_i \times \kappa_i}$ and $b_i \in \mathbb{R}^{\kappa_i}$ are expressed by:

$$\Delta_i = \begin{bmatrix} 0 & 1 & \dots & 0 \\ \vdots & \vdots & \ddots & \vdots \\ 0 & 0 & 0 & 1 \\ 0 & 0 & 0 & 0 \end{bmatrix}, b_i = \begin{bmatrix} 0 \\ \vdots \\ 0 \\ 1 \end{bmatrix}, \tag{43}$$

with κ_i, for $i = 1, \dots, \nu = \mathrm{rank}(B)$ are the controllability indices of the system as defined by Rosenbrock[28] and Sontag.[31] These controllability indices must verify: $\sum_{i=1}^{\nu} \kappa_i = n$.

This state space is obtained thanks to the feedback transformation:

$$\begin{aligned} \bar{x} &= Mx, \\ \bar{u} &= Kx + Lu \end{aligned} \tag{44}$$

DOI: 10.13009/EUCASS2019-713

The flat output $z = [z_1 \ \dots \ z_\nu]^T$ of the linear system (40) are its Brunovskii output that is described by:

$$z = \bar{C}\bar{x}, \quad \text{where} \quad \bar{C} = \text{diag}(\Lambda_1, \dots, \Lambda_\nu), \tag{45}$$

with $\Lambda_i \in \mathbb{R}^{1\times\kappa_i}$ such that:

$$\Lambda_i = \begin{bmatrix} 1 & 0 & \dots & 0 \end{bmatrix}. \tag{46}$$

Noting that:

$$\bar{x} = \begin{bmatrix} z_1 \\ \vdots \\ z_1^{(\kappa_1)} \\ \vdots \\ z_\nu \\ \vdots \\ z_\nu^{(\kappa_\nu)} \end{bmatrix}, \quad \bar{u} = \begin{bmatrix} z_1^{(\kappa_1+1)} \\ \vdots \\ z_\nu^{(\kappa_\nu+1)} \end{bmatrix}, \quad \text{and} \quad \bar{z} = \begin{bmatrix} \bar{x} \\ \bar{u} \end{bmatrix}, \tag{47}$$

the original state vector x and the input vector u are computed in terms of the flat output z and its derivatives by inverting (44):

$$\begin{aligned} x &= M^{-1}\bar{x} = \begin{bmatrix} M^{-1} & 0 \end{bmatrix} \bar{z}, \\ u &= L^{-1}K\bar{x} + L^{-1}\bar{u} = \begin{bmatrix} L^{-1}K & L^{-1} \end{bmatrix} \bar{z}. \end{aligned} \tag{48}$$

In the case of the dynamics (8) this procedure is applied to obtain a Brunovskii form such that the pair $(\tilde{A}, \tilde{B})$ is controllable. In that case, $\nu = \text{rank}(B) = 3$ and the controllability indices are $\kappa_1 = \kappa_2 = \kappa_3 = 2$. It comes that the matrices M, K and L can be computed such that the state vector $\bar{\zeta}$ verifies:

$$\dot{\bar{\zeta}} = \bar{A}\bar{\zeta} + \bar{D} + \bar{B}\bar{u} \tag{49}$$

Matrices $\bar{A}$ and $\bar{B}$ satisfy the Brunovskii characteristics:

$$\bar{A} = \begin{bmatrix} 0 & 1 & 0 & 0 & 0 & 0 \\ 0 & 0 & 0 & 0 & 0 & 0 \\ 0 & 0 & 0 & 1 & 0 & 0 \\ 0 & 0 & 0 & 0 & 0 & 0 \\ 0 & 0 & 0 & 0 & 0 & 1 \\ 0 & 0 & 0 & 0 & 0 & 0 \end{bmatrix}, \quad \bar{B} = \begin{bmatrix} 0 & 0 & 0 \\ 1 & 0 & 0 \\ 0 & 0 & 0 \\ 0 & 1 & 0 \\ 0 & 0 & 0 \\ 0 & 0 & 1 \end{bmatrix}, \quad \bar{D} = \begin{bmatrix} \bar{d}_1 \\ \bar{d}_2 \\ \bar{d}_3 \\ \bar{d}_4 \\ \bar{d}_5 \\ \bar{d}_6 \end{bmatrix} \quad \text{and} \quad \bar{C} = \begin{bmatrix} 1 & 0 & 0 & 0 & 0 & 0 \\ 0 & 0 & 1 & 0 & 0 & 0 \\ 0 & 0 & 0 & 0 & 1 & 0 \end{bmatrix} \tag{50}$$

As opposed to the system under Brunovskii form (41), the system given by Equation (49) has a drift term. This term is removed by means of the following time varying transformation:

$$\begin{aligned} z_1 &= \bar{\zeta}_1 - \bar{d}_1(t - t_0) - \frac{1}{2}\bar{d}_2(t - t_0)^2, \\ \dot{z}_1 &= \bar{\zeta}_2 - \bar{d}_2(t - t_0), \\ \ddot{z}_1 &= \bar{u}_1, \\ z_2 &= \bar{\zeta}_3 - \bar{d}_3(t - t_0) - \frac{1}{2}\bar{d}_4(t - t_0)^2, \\ \dot{z}_2 &= \bar{\zeta}_4 - \bar{d}_4(t - t_0), \\ \ddot{z}_2 &= \bar{u}_2, \\ z_3 &= \bar{\zeta}_5 - \bar{d}_5(t - t_0) - \frac{1}{2}\bar{d}_6(t - t_0)^2, \\ \dot{z}_3 &= \bar{\zeta}_3 - \bar{d}_6(t - t_0), \\ \ddot{z}_2 &= \bar{u}_3. \end{aligned} \tag{51}$$

Doing so, the vector $z = [z_1 \ z_2 \ z_3]^T$ is the flat output of the system (8). With the vector $\bar{z}$ defined as:

$$\bar{z} = \begin{bmatrix} z_1 & \dot{z}_1 & z_2 & \dot{z}_2 & z_3 & \dot{z}_3 & \ddot{z}_1 & \ddot{z}_2 & \ddot{z}_3 \end{bmatrix}^T, \tag{52}$$

DOI: 10.13009/EUCASS2019-713

the transformation (51) is rewritten in matrix form as:

$$\bar{z} = \begin{bmatrix} \bar{\zeta} - \bar{\zeta}_D(t) \\ \bar{u} \end{bmatrix} \tag{53}$$

The state $\bar{\zeta}$ and the input $\bar{u}$ are recovered the flat output and its successives derivatives by inverting Equation (51) defining the flat outputs:

$$\begin{aligned}
\bar{\zeta}_1 &= z_1 + \bar{d}_1(t-t_0) + \frac{1}{2}\bar{d}_2(t-t_0)^2,\\
\bar{\zeta}_2 &= \dot{z}_1 + \bar{d}_2(t-t_0),\\
\bar{\zeta}_3 &= z_2 + \bar{d}_3(t-t_0) + \frac{1}{2}\bar{d}_4(t-t_0)^2,\\
\bar{\zeta}_4 &= \dot{z}_2 + \bar{d}_4(t-t_0),\\
\bar{\zeta}_5 &= z_3 + \bar{d}_5(t-t_0) + \frac{1}{2}\bar{d}_6(t-t_0)^2,\\
\bar{\zeta}_6 &= \dot{z}_3 + \bar{d}_6(t-t_0),\\
\bar{u}_1 &= \ddot{z}_1,\\
\bar{u}_2 &= \ddot{z}_2,\\
\bar{u}_3 &= \ddot{z}_3.
\end{aligned} \tag{54}$$

Applying then (48) leads to the original state and control vectors ζ and u.

3.3 Flat optimal control problem

In this section, the optimal control problem (1) is transformed into a linear program. This transformation is executed by means of three step:

i set the genuine optimal control problem (1) in terms of flat outputs;

ii parametrize the flat outputs using B-splines basis;

iii discretize the constraints.

The interest of expressing the Problem (1) in terms of the flat output comes from a twofold fact. First, the differential flatness ensures a Lie-Backlünd equivalence between the original system (8) and its Brunovskii form (49). Moreover, for any flat system, any sufficiently smooth function $t \mapsto z(t)$ leads to time state trajectories $t \mapsto (\zeta(t), u(t))$ that satisfy the dynamic equation (8) and consequently (5). With these two arguments, the OCP (1) can be recast using the $\bar{z}$ coordinates instead of (ζ, u). Doing so, the dynamic constraint is removed since it is always satisfied by any given trajectory $t \mapsto \bar{z}(t)$. Consequently, the optimal control problem boils down to a geometric problem of finding a time-parametrized curve in the $\bar{z}$-space that links two points (initial and final conditions) while belonging to S_z a given subspace of $\bar{z}$:

$$\begin{matrix} \min\limits_{\bar{z}} J(\bar{z}) \\ \text{s. t.:} \end{matrix} \quad \begin{cases} \bar{z}(t_0) \text{ fixed} \\ \bar{z}(t_f) \text{ free} \\ \bar{z}(t) \in S_z \end{cases} \tag{55}$$

The subset S_z is defined by the path and control constraints $\gamma(\cdot)$ such that

$$S_z = \{\bar{z} | \, \gamma_z(\bar{z}(t)) \leq 0\}. \tag{56}$$

with the function $\gamma_z(\bar{z}(t))$ defined by the following set of inequality constraints:

$$\begin{cases} \left\| \begin{bmatrix} 0 & 1 & 0 \\ 0 & 0 & 1 \end{bmatrix} C(t)W(t) \begin{bmatrix} M^{-1} & 0 \end{bmatrix} \bar{z}(t) \right| \leqslant \delta_2, \\ \left\| \begin{bmatrix} L^{-1}K & L^{-1} \end{bmatrix} \bar{z}(t) \right| \leqslant U_{\max}, \end{cases} \quad \forall t \in [t_0, t_1], \tag{57}$$

Using flatness property of the system, the dynamic constraint of the optimal control problem has been removed. Nevertheless, problem (55) remains a difficult problem due to the infinite dimensions of the problem. To deal with the infinite dimension of the problem (55), a B-splines collocation method (Hargraves[15]) is applied to transform problem

DOI: 10.13009/EUCASS2019-713

(55) into a computationally tractable linear programming (LP) (see Neckel[27] and Milam[25]). Contrary to the polynomials, the choice of the B-splines allows us to define flexible trajectories with high continuity level using a low number of parameters.

This method consists in parametrizing the flat output z components such that:

$$z_i(t) = \sum_{j=1}^{n} \alpha_{i,j} B_{j,k}(t), \qquad i = 1,2,3 \tag{58}$$

where the $B_{j,k}$ are a k^{th} order B-splines basis of the piecewise polynomials of degree at most $k-1$ built on the breakpoints sequence $\{t_i\}_{i=1}^{p+1}$ such that

$$t_0 = t_1 < t_2 < \cdots < t_p < t_{p+1} = t_f. \tag{59}$$

Thereby, the knots sequence $\mathcal{T} = \{t_i\}$ is chosen to ensure a maximum continuity at interior knots:

$$\mathcal{T} = \{\underbrace{t_1, \ldots, t_1}_{k \text{ times}}, t_2, t_3, \ldots, t_{p-1}, \underbrace{t_p, \ldots, t_p}_{k \text{ times}}\}. \tag{60}$$

B-splines are defined by the Cox-de Boor iterative algorithm (Lee[18]). The $\alpha_{i,j}$ coefficients are called control points. After parametrization of flat outputs, the vector of all control points

$$\alpha = (\alpha_{1,1}, \ldots, \alpha_{1,n}, \alpha_{2,1}, \ldots, \alpha_{2,n}, \alpha_{3,1}, \ldots, \alpha_{3,n}) \tag{61}$$

becomes the decision variable in the optimization problem.

Equation (58) and its derivatives up to order 2 can be rewritten in matrix form:

$$\begin{bmatrix} z_1(t) \\ \dot{z}_1(t) \\ \ddot{z}_1(t) \\ z_2(t) \\ \dot{z}_2(t) \\ \ddot{z}_2(t) \\ z_3(t) \\ \dot{z}_3(t) \\ \ddot{z}_3(t) \end{bmatrix} = \begin{bmatrix} B_{1,k}(t) & \ldots & B_{n,k}(t) & 0 & \ldots & \ldots & \ldots & \ldots & 0 \\ \dot{B}_{1,k}(t) & \ldots & \dot{B}_{n,k}(t) & 0 & \ldots & \ldots & \ldots & \ldots & 0 \\ \ddot{B}_{1,k}(t) & \ldots & \ddot{B}_{n,k}(t) & 0 & \ldots & \ldots & \ldots & \ldots & 0 \\ 0 & \ldots & 0 & B_{1,k}(t) & \ldots & B_{n,k}(t) & 0 & \ldots & 0 \\ 0 & \ldots & 0 & \dot{B}_{1,k}(t) & \ldots & \dot{B}_{n,k}(t) & 0 & \ldots & 0 \\ 0 & \ldots & 0 & \ddot{B}_{1,k}(t) & \ldots & \ddot{B}_{n,k}(t) & 0 & \ldots & 0 \\ 0 & \ldots & \ldots & \ldots & \ldots & 0 & B_{1,k}(t) & \ldots & B_{n,k}(t) \\ 0 & \ldots & \ldots & \ldots & \ldots & 0 & \dot{B}_{1,k}(t) & \ldots & \dot{B}_{n,k}(t) \\ 0 & \ldots & \ldots & \ldots & \ldots & 0 & \ddot{B}_{1,k}(t) & \ldots & \ddot{B}_{n,k}(t) \end{bmatrix} \alpha, \tag{62}$$

and after reordering:

$$\bar{z}(t) = R(t)\alpha. \tag{63}$$

Doing so, the relative equinoctial orbital elements are computed as:

$$\begin{aligned} x(t) &= W(t) \begin{bmatrix} M^{-1} & 0_{6\times3} \end{bmatrix} \begin{bmatrix} \bar{\zeta} \\ \bar{u} \end{bmatrix} \\ &= W(t) \begin{bmatrix} M^{-1} & 0_{6\times3} \end{bmatrix} \left(\bar{z} + \begin{bmatrix} \bar{\zeta}_D(t) \\ 0_{3\times1} \end{bmatrix} \right) \\ &= W(t) \begin{bmatrix} M^{-1} & 0_{6\times3} \end{bmatrix} \left(R(t)\alpha + \begin{bmatrix} \bar{\zeta}_D(t) \\ 0_{3\times1} \end{bmatrix} \right) \\ &= W(t) \begin{bmatrix} M^{-1} & 0_{6\times3} \end{bmatrix} R(t)\alpha + W(t) M^{-1} \bar{\zeta}_D(t), \end{aligned} \tag{64}$$

and the relative geographical position is given by:

$$y(t) = C_{\varphi\lambda} W(t) \begin{bmatrix} M^{-1} & 0_{6\times3} \end{bmatrix} R(t)\alpha + C_{\varphi\lambda} W(t) M^{-1} \bar{\zeta}_D(t). \tag{65}$$

The SK constraint (35) is then transformed in the two following linear constraints:

$$\begin{cases} C_{\varphi\lambda} W(t) \begin{bmatrix} M^{-1} & 0_{6\times3} \end{bmatrix} R(t)\alpha \leqslant \delta_2 - C_{\varphi\lambda} W(t) M^{-1} \bar{\zeta}_D(t), \\ -C_{\varphi\lambda} W(t) \begin{bmatrix} M^{-1} & 0_{6\times3} \end{bmatrix} R(t)\alpha \leqslant \delta_2 + C_{\varphi\lambda} W(t) M^{-1} \bar{\zeta}_D(t) \end{cases} \tag{66}$$

DOI: 10.13009/EUCASS2019-713

Likewise, the control created by the satellite thrusters is expressed as:

$$\begin{aligned} u(t) &= \begin{bmatrix} L^{-1}K & L^{-1} \end{bmatrix} \begin{bmatrix} \bar{\zeta} \\ \bar{u} \end{bmatrix} \\ &= \begin{bmatrix} L^{-1}K & L^{-1} \end{bmatrix} \left(\bar{z} + \begin{bmatrix} \bar{\zeta}_D(t) \\ 0_{3\times 1} \end{bmatrix} \right) \\ &= \begin{bmatrix} L^{-1}K & L^{-1} \end{bmatrix} \bar{z} + L^{-1}K\bar{\zeta}_D(t) \\ &= \begin{bmatrix} L^{-1}K & L^{-1} \end{bmatrix} R(t)\alpha + L^{-1}K\bar{\zeta}_D(t), \end{aligned} \tag{67}$$

and the constraint (36) is transformed to:

$$\begin{cases} \begin{bmatrix} L^{-1}K & L^{-1} \end{bmatrix} R(t)\alpha \leqslant U_{\max} - L^{-1}K\bar{\zeta}_D(t), \\ -\begin{bmatrix} L^{-1}K & L^{-1} \end{bmatrix} R(t)\alpha \leqslant U_{\max} + L^{-1}K\bar{\zeta}_D(t) \end{cases} \tag{68}$$

The constraints are enforced at a finite number of points $\{\tau_j\}_{j=1,\dots,N_C}$ named collocation points. The choice of $\{\tau_j\}$ is then also a degree of freedom in the path planning design process. The descritize constraints read:

$$\begin{cases} C_{\varphi\lambda}W(\tau_j)\begin{bmatrix} M^{-1} & 0_{6\times 3} \end{bmatrix} R(\tau_j)\alpha \leqslant \delta_2 - C_{\varphi\lambda}W(\tau_j)M^{-1}\bar{\zeta}_D(\tau_j), \\ -C_{\varphi\lambda}W(\tau_j)\begin{bmatrix} M^{-1} & 0_{6\times 3} \end{bmatrix} R(\tau_j)\alpha \leqslant \delta_2 + C_{\varphi\lambda}W(\tau_j)M^{-1}\bar{\zeta}_D(\tau_j) \\ \begin{bmatrix} L^{-1}K & L^{-1} \end{bmatrix} R(\tau_j)\alpha \leqslant U_{\max} - L^{-1}K\bar{\zeta}_D(\tau_j), \\ -\begin{bmatrix} L^{-1}K & L^{-1} \end{bmatrix} R(\tau_j)\alpha \leqslant U_{\max} + L^{-1}K\bar{\zeta}_D(\tau_j), \end{cases} \qquad \forall j = 1, \dots, N_C. \tag{69}$$

The objective function (37) is also discretized in the following way:

$$\begin{aligned} J(u) &= \int_{t_0}^{t_1} |u(t)| dt, \\ &= \int_{t_0}^{t_1} \left(|u_R(t)| + |u_T(t)| + |u_N(t)| \right) dt, \\ &= \frac{t_1 - t_0}{N_C} \sum_{j=1}^{N_C} \left(|u_R(\tau_j)| + |u_T(\tau_j)| + |u_N(\tau_j)| + |u_R(\tau_{j+1})| + |u_T(\tau_{j+1})| + |u_N(\tau_{j+1})| \right). \end{aligned} \tag{70}$$

In Equation (70), the control unknowns do not appear linearly, but with absolute values. In order to remove the absolute values, auxiliary variables $\{w_{R_j}, w_{T_j}, w_{N_j}\}_{j=1,\dots,N_C}$ are used, defining a new objective function:

$$\tilde{J}(w_{R_j}, w_{T_j}, w_{N_j}) = \sum_{j=1}^{N_C} (w_{R_j} + w_{R_{j+1}} + w_{T_j} + w_{T_{j+1}} + w_{N_j} + w_{N_{j+1}}), \tag{71}$$

with new constraints for these auxiliary variables:

$$\begin{cases} u(\tau_j) - w_j \leqslant 0, \\ -u(\tau_j) - w_j \leqslant 0, \end{cases} \qquad \text{with } w_j = \begin{bmatrix} w_{R_j} \\ w_{T_j} \\ w_{N_j} \end{bmatrix}, \ \forall j = 1, \dots, N_C, \tag{72}$$

that can also be rewritten as:

$$\begin{cases} \begin{bmatrix} L^{-1}K & L^{-1} \end{bmatrix} R(\tau_j)\alpha - w_j \leqslant -L^{-1}K\bar{\zeta}_D(\tau_j), \\ -\begin{bmatrix} L^{-1}K & L^{-1} \end{bmatrix} R(\tau_j)\alpha - w_j \leqslant L^{-1}K\bar{\zeta}_D(\tau_j), \end{cases} \qquad \forall j = 1, \dots, N_C. \tag{73}$$

The vector of decision variables is augmen The auxiliary variables w_j are new unknowns and are added to the vector of decision variables. The augmented vector is:

$$\bar{\alpha} = \begin{bmatrix} \alpha & w_{R_1} & \dots & w_{R_{N_C}} & w_{T_1} & \dots & w_{N_{N_C}} \end{bmatrix}^T \in \mathbb{R}^{3n+3N_C} \tag{74}$$

A last constraint is added in order to ensure that the trajectory starts at the given initial point. If x_0 is the initial point, the boundary constraint reads:

$$W(t_0)\begin{bmatrix} M^{-1} & 0_{6\times 3} \end{bmatrix} R(t_0)\alpha = x_0 - W(t)M^{-1}\bar{\zeta}_D(t_0). \tag{75}$$

Finally, associated with B-splines collocation method, the flat optimal control problem can be stated as the following linear programming problem:

DOI: 10.13009/EUCASS2019-713

Problem 2

$$\min_{\bar{\alpha}} \tilde{J}(\bar{\alpha}) \quad \text{s. t.:} \quad \forall j = 1, \ldots, N_C : \begin{cases} C_{\varphi\lambda} W(\tau_j) \begin{bmatrix} M^{-1} & 0_{6\times 3} \end{bmatrix} R(\tau_j)\alpha \leqslant \delta_2 - C_{\varphi\lambda} W(\tau_j) M^{-1} \bar{\zeta}_D(\tau_j), \\ -C_{\varphi\lambda} W(\tau_j) \begin{bmatrix} M^{-1} & 0_{6\times 3} \end{bmatrix} R(\tau_j)\alpha \leqslant \delta_2 + C_{\varphi\lambda} W(\tau_j) M^{-1} \bar{\zeta}_D(\tau_j) \\ \begin{bmatrix} L^{-1}K & L^{-1} \end{bmatrix} R(\tau_j)\alpha \leqslant U_{\max} - L^{-1}K\bar{\zeta}_D(\tau_j), \\ -\begin{bmatrix} L^{-1}K & L^{-1} \end{bmatrix} R(\tau_j)\alpha \leqslant U_{\max} + L^{-1}K\bar{\zeta}_D(\tau_j), \\ \begin{bmatrix} L^{-1}K & L^{-1} \end{bmatrix} R(\tau_j)\alpha - w_j \leqslant -L^{-1}K\bar{\zeta}_D(\tau_j), \\ -\begin{bmatrix} L^{-1}K & L^{-1} \end{bmatrix} R(\tau_j)\alpha - w_j \leqslant L^{-1}K\bar{\zeta}_D(\tau_j), \\ W(t_0) \begin{bmatrix} M^{-1} & 0_{6\times 3} \end{bmatrix} R(t_0)\alpha = x_0 - W(t) M^{-1} \bar{\zeta}_D(t_0) \end{cases} \tag{76}$$

◦

The latter problem shows the advantages of being linear and integration-free, what makes it numerically tractable.

4. Numerical results

The proposed transformation of the GEO SK fuel optimization problem into a linear programming problem is applied on a 4000 kg satellite equipped with an electric propulsion system consisting of one thruster on each face producing a maximum thrust level of 0.2 N each. The station keeping mean longitude is chosen to be $\ell_{M\Theta,sk} = 218°$ and the half-width SK window is equal to 0.5°. Therefore, the dynamic matrix of the LTI system (8) can be numericaly evaluated as:

$$\tilde{A} = \begin{bmatrix} 4.73 & -3.15 & -6.30 & 8.58\ 10^{-10} & 0 & 1.58 \\ -2.36 & 1.58 & -6.30 & -6.27\ 10^{-10} & 0 & -7.88\ 10^{-1} \\ 1.89\ 10^{1} & -1.26\ 10^{1} & -2.82\ 10^{-5} & -8.84\ 10^{-10} & -2.16\ 10^{-9} & 9.40\ 10^{-6} \\ -1.28\ 10^{-9} & 1.28\ 10^{-9} & 0 & 0 & -6.30 & 0 \\ -3.65\ 10^{-11} & -1.23\ 10^{-10} & -9.57\ 10^{-10} & 6.30 & 1.57\ 10^{-6} & -1.60\ 10^{-10} \\ -1.89\ 10^{1} & 1.26\ 10^{1} & 6.30 & -4.86\ 10^{-9} & -2.55\ 10^{-9} & -6.30 \end{bmatrix} \tag{77}$$

$$\tilde{D} = \begin{bmatrix} -1.40\ 10^{-3} & -1.76\ 10^{-3} & -6.26\ 10^{-6} & 0 & -2.70\ 10^{-10} & 6.99\ 10^{-4} \end{bmatrix}^T \tag{78}$$

Althoug the analytical expression of the dynamics is available, the litteral computation of the transformation matrices M, K and L to obtain the flat outputs is too tedious and is not analytically tractable. However, these matrices, as well as the initial dynamics matrices, depend only on the station keeping longitude that is fixed for a given spacecraft mission. The numerical expression of these matrices is:

$$M = \begin{bmatrix} -1.32\ 10^{-5} & 0 & -1.59\ 10^{-1} & 0 & 0 & 0 \\ -3.00 & 2.00 & 8.74\ 10^{-5} & 0 & 2.17\ 10^{-8} & -2.22\ 10^{-5} \\ -3.17\ 10^{-1} & 0 & -1.18\ 10^{-7} & 0 & 0 & 0 \\ -1.50 & 1.00 & 2.00 & 0 & 0 & -5.00\ 10^{-1} \\ 0 & 0 & 0 & -3.17\ 10^{-1} & 0 & 0 \\ 0 & 0 & 0 & 0 & 2.00 & 0 \end{bmatrix} \tag{79}$$

$$K = \begin{bmatrix} -1.89\ 10^{1} & 1.26\ 10^{1} & 6.30 & 1.33\ 10^{-7} & 0 & -6.30 \\ 3.78\ 10^{1} & -2.52\ 10^{1} & 1.56\ 10^{-6} & 0 & 0 & 2.35\ 10^{-6} \\ 0 & 0 & 0 & 1.26\ 10^{1} & 3.13\ 10^{-6} & 0 \end{bmatrix} \tag{80}$$

$$L = \begin{bmatrix} 1 & 4.44\ 10^{-5} & 0 \\ 0 & 1 & 0 \\ 0 & 0 & 1 \end{bmatrix} \tag{81}$$

Problem 2 is solved with a B-spline basis of degree 5 and 25 collocation points. Besides this, the time grid used for the evaluation of the constraints ranges from 0 to 10 days with 500 points. The initial relative state vector chosen for this study is:

$$x_0 = \begin{bmatrix} 0 & 0 & 0 & 0 & 1.10^{-4} & 0 \end{bmatrix}^T. \tag{82}$$

The flat outputs and their derivatives are displayed on Figures 1, 2 and 3 for z_1, z_2 and z_3 respectively, as well as their derivatives. The oscillations observed on the curves come from the high degree chosen for the basis of splines function that lead to the control profile skeched on Figure 4. For a time horizon of 10 days, the Δv requirement is 1.10 m/s.

DOI: 10.13009/EUCASS2019-713

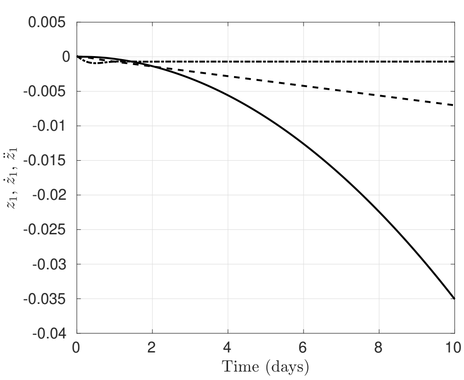

Figure 1: Flat output z_1 with its first and second derivatives: –: $z_1(t)$, - -: $\dot{z}_1(t)$, $- \cdot -$: $\ddot{z}_1(t)$.

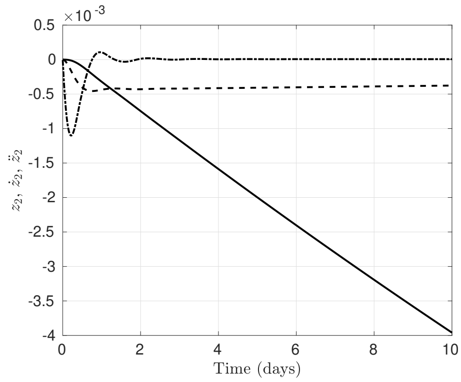

Figure 2: Flat output z_2 with its first and second derivatives: –: $z_2(t)$, - -: $\dot{z}_2(t)$, $- \cdot -$: $\ddot{z}_2(t)$.

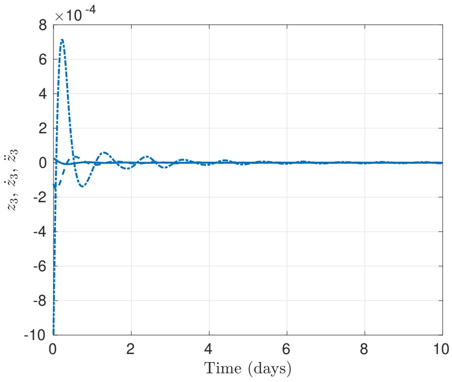

Figure 3: Flat output z_3 with its first and second derivatives: –: $z_3(t)$, - -: $\dot{z}_3(t)$, $- \cdot -$: $\ddot{z}_3(t)$.

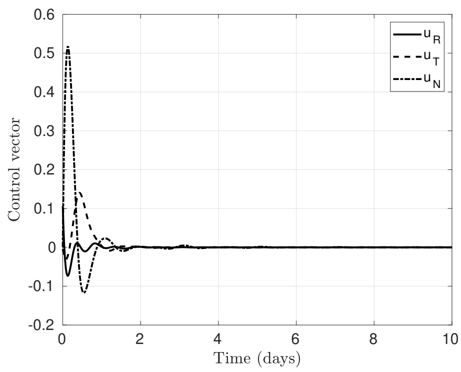

Figure 4: Control profile.

The Figure 5 shows the spacecraft trajectory with the SK window. From Soop,[32] it is well known that the C_{22} and S_{22} terms of the potential steer the satellite away from its SK position. Spacecraft with a longitude equal to 118° tend to drift eastwards (the longitude decreases). The Figure 5 shows that the best way to control the spacecraft is to drive it to the west part of the Sk window and let it drift toward the east direction. at the end of the SK horizon.

DOI: 10.13009/EUCASS2019-713

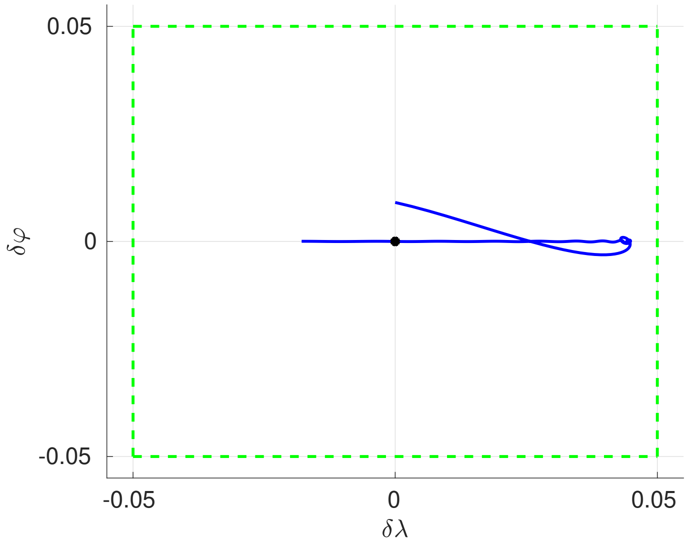

Figure 5: Trajectory of the spacecraft in the station keeping window. $*$: initial point.

5. Conclusion

In this paper, the dynamic geostationary station-keeping problem for a satellite undergoing Earth non-spherical perturbation potential harmonics up to degree and order 2 has been transformed to a linear optimization problem thanks to two transformations. The first one involves the Floquet-Lyapunov theory for transforming a periodic bounded linear time varying system in a linear time invariant system. The second transformation aims at transforming the previously computed linear system in its Brunovskii canonical form. The novelty of our approach is to have designed a time varying flat output expression for removing the constant drifting term of the relative geostationary dynamics. The flats outputs have been parametrized by B-splines. The linear transformed station keeping problem has been solved for a realistic telecommunication stallite equipped with an ideal propulsion system with one thruster mounted on each face of the satellite.

A. Disturbing Gravitational Potential of the Earth

Kaula [**?**, chapter 3] derives the expression of the Legendre decomposition of the Earth disturbing potential. The proposed study requires to compute these coefficients up to degree and order 2 in terms of the equinoctial orbital elements defined by Equation 1.

In the following expressions, μ is the gravitational geocentric parameter and R_e the mean Earth radius. In order shorten the expression of the potentials, the following variables are used:

$$\begin{cases} C_{n\kappa+m\Theta} = \cos\Big(n\kappa_{sk}(t) + m\Theta(t)\Big), \\ S_{n\kappa+m\Theta} = \sin\Big(n\kappa_{sk}(t) + m\Theta(t)\Big), \end{cases} \quad \text{with } \kappa_{sk}(t) = \ell_{M\Theta,sk} + \Theta(t), \quad \text{for } n \text{ and } m \text{integers.} \tag{83}$$

$$\begin{cases} C_{n\ell} = \cos\Big(n\ell_{M\Theta,sk}\Big), \\ S_{n\ell} = \sin\Big(n\ell_{M\Theta,sk}\Big), \end{cases} \quad \text{for } n \text{ an integer.} \tag{84}$$

DOI: 10.13009/EUCASS2019-713

The potential term of degree 2 and order 0, also known as the J_2 term, reads:

$$
\begin{aligned}
V_{C_{20}}(x_{eoe}) = \frac{\mu R_e^2 C_{20}}{a^3}\Bigg\{ & \left[\frac{3(i_x^2+i_y^2)}{(1+i_x^2+i_y^2)^2}-\frac{1}{2}\right]\Bigg[\left(3+\frac{27}{8}(e_x^2+e_y^2)\right)(e_xC_\kappa+e_yS_\kappa) \\
& \left(\frac{9}{2}+\frac{7}{2}(e_x^2+e_y^2)\right)((e_x^2-e_y^2)C_{2\kappa}+2e_xe_yS_{2\kappa})\Bigg] \\
& -\frac{3}{2}\frac{1}{(1+i_x^2+i_y^2)^2}\Bigg[\left(-1+\frac{1}{8}(e_x^2+e_y^2)\right)\Big((i_x^2-i_y^2)(e_xC_\kappa-e_yS_\kappa)+2i_xi_y(e_yC_\kappa+e_xS_\kappa)\Big) \\
& \left(2-5(e_x^2+e_y^2)+\frac{13}{8}(e_x^2+e_y^2)^2\right)((i_x^2-i_y^2)C_{2\kappa}+2i_xi_yS_{2\kappa}) \\
& \left(7-\frac{123}{8}(e_x^2+e_y^2)\right)\Big([e_x(i_x^2-i_y^2)-2e_yi_xi_y]C_{3\kappa}+[e_y(i_x^2-i_y^2)+2e_xi_xi_y]S_{3\kappa}\Big) \\
& \left(17-\frac{115}{3}(e_x^2+e_y^2)\right)\Big(-[4e_xe_yi_xi_y-(e_x^2-e_y^2)(i_x^2-i_y^2)]C_{4\kappa}+2[e_xe_y(i_x^2-i_y^2)+i_xi_y(e_x^2-e_y^2)]S_{4\kappa}\Big)\Bigg]\Bigg\}
\end{aligned} \tag{85}
$$

with C_{20} the Earth gravitational potential Legendre coefficient of degree 2 and order 0. Its value is given in Appendix C.

The potential terms of degree 2 and order 1 read:

$$
\begin{aligned}
V_{C_{21}}(x_{eoe}) = {} & \frac{\mu R_e^2 C_{21}}{a^3}\frac{3}{(1+i_x^2+i_y^2)^2}\Bigg\{ \\
& \left[\frac{9}{4}+\frac{7}{4}(e_x^2+e_y^2)\right]\Bigg[-i_y(3i_x^2-iy^2+1)C_\theta\Big(\big(C_{4\kappa}+1\big)(e_x^2-e_y^2)+2e_xe_yS_{4\kappa}\Big) \\
& \quad +i_x(i_x^2-3i_y^2+1)C_\theta\Big(-2e_xe_y\big(C_{4\kappa}-1\big)+(e_x^2-e_y^2)S_{4\kappa}\Big) \\
& \quad -2i_y(3i_x^2-iy^2-1)S_\theta e_xe_y\,(C_{4\kappa}+S_{4\kappa}-1) \\
& \quad +i_x(i_x^2-3i_y^2-1)S_\theta(e_x^2-e_y^2)\,(C_{4\kappa}+S_{4\kappa}+1) \\
& \quad +2(i_x^2+i_y^2-1)(i_yC_\theta-i_xS_\theta)\Big((e_x^2-e_y^2)C_{2\kappa}+2e_xe_yS_{2\kappa}\Big)\Bigg] \\
& +\left[\frac{3}{2}+\frac{27}{16}(e_x^2+e_y^2)\right]\Bigg[\Big[i_x(i_x^2-3i_y^2+1)C_\theta+i_y(3i_x^2-i_y^2-1)S_\theta\Big]\Big[e_y\big(-C_{3\kappa}+C_\kappa\big)+e_x\big(S_{3\kappa}+S_\kappa\big)\Big] \\
& \quad +\Big[i_x(i_x^2-3i_y^2-1)S_\theta-i_y(3i_x^2-i_y^2+1)C_\theta\Big]\Big[e_xC_{3\kappa}+e_yS_{3\kappa}\Big] \\
& \quad -e_xC_\kappa\Big[i_y\big(i_x^2-3i_y^2+3\big)C_\theta+i_x\big(i_x^2+5i_y^2-1\big)S_\theta\Big] \\
& \quad +e_yS_\kappa\Big[i_y\big(5i_x^2+i_y^2-1\big)C_\theta-i_x\big(3i_x^2-i_y^2-3\big)S_\theta\Big]\Bigg] \\
& +\frac{1}{(1-e_x^2-e_y^2)^{\frac{3}{2}}}\Bigg[C_{2\kappa}\Big(i_y(i_y^2-3i_x^2-1)C_\theta+i_x(i_x^2-3i_y^2-1)S_\theta\Big) \\
& \quad +S_{2\kappa}\Big(i_x(i_x^2-3i_y^2+1)C_\theta-i_y(i_y^2-3i_x^2+1)S_\theta\Big) \\
& \quad +(i_x^2+i_y^2-1)(i_yC_\theta-i_xS_\theta)\Bigg]\Bigg\}
\end{aligned} \tag{86}
$$

DOI: 10.13009/EUCASS2019-713

and:

$$
\begin{aligned}
V_{S_{21}}(x_{eoe}) = \frac{\mu R_e^2 S_{21}}{a^3}\frac{3}{(1+i_x^2+i_y^2)^2}\Bigg\{ & \\
&\left[\frac{9}{4}+\frac{7}{4}(e_x^2+e_y^2)\right]\Bigg[i_y(3i_x^2-iy^2-1)C_\theta\left(-2e_xe_y\left(C_{4\kappa}-1\right)+(e_x^2-e_y^2)S_{4\kappa}\right)\\
&\quad + i_x(i_x^2-3i_y^2-1)C_\theta\left((e_x^2-e_y^2)\left(C_{4\kappa}-1\right)+2e_xe_yS_{4\kappa}\right)\\
&\quad + i_y(3i_x^2-iy^2+1)S_\theta(e_x^2-e_y^2)\left(C_{4\kappa}+S_{4\kappa}+1\right)\\
&\quad + 2i_x(i_x^2-3i_y^2+1)S_\theta e_xe_y\left(C_{4\kappa}+S_{4\kappa}-1\right)\\
&\quad - 2(i_x^2+i_y^2-1)(i_xC_\theta+i_yS_\theta)\left((e_x^2-e_y^2)C_{2\kappa}+2e_xe_yS_{2\kappa}\right)\Bigg]\\
&+\left[\frac{3}{2}+\frac{27}{16}(e_x^2+e_y^2)\right]\Bigg[\left[i_y(3i_x^2-i_y^2-1)C_\theta-i_x(i_x^2-3i_y^2+1)S_\theta\right]\left[e_y\Big(-C_{3\kappa}+C_\kappa\Big)+e_x\Big(S_{3\kappa}+S_\kappa\Big)\right]\\
&\quad +\left[i_x(i_x^2-3i_y^2-1)C_\theta+i_y(3i_x^2-i_y^2+1)S_\theta\right]\left[e_xC_{3\kappa}+e_yS_{3\kappa}\right]\\
&\quad - e_xC_\kappa\left[i_y\Big(i_x^2-3i_y^2+3\Big)S_\theta-i_x\Big(i_x^2+5i_y^2-1\Big)C_\theta\right]\\
&\quad + e_yS_\kappa\left[i_x\Big(3i_x^2-i_y^2-3\Big)C_\theta-i_y\Big(5i_x^2+i_y^2-1\Big)S_\theta\right]\Bigg]\\
&+\frac{1}{(1-e_x^2-e_y^2)^{\frac{3}{2}}}\Bigg[C_{2\kappa}\Big(i_x(i_x^2-3i_y^2-1)C_\theta-i_y(i_y^2-3i_x^2-1)S_\theta\Big)\\
&\quad - S_{2\kappa}\Big(i_y(i_y^2-3i_x^2+1)C_\theta+i_x(i_x^2-3i_y^2+1)S_\theta\Big)\\
&\quad - (i_x^2+i_y^2-1)(i_xC_\theta+i_yS_\theta)\Bigg]\Bigg\}
\end{aligned}
\tag{87}
$$

with C_{21} and S_{21} the Earth gravitational potential Legendre coefficients of degree 2 and order 1. Their values are given in Appendix C.

The potential terms of degree 2 and order 2, read:

$$
\begin{aligned}
V_{C_{22}}(x_{eoe}) = \frac{\mu R_e^2 C_{22}}{a^3}\frac{3}{(1+i_x^2+i_y^2)^2}\Bigg\{ & \\
&\left[-\frac{1}{2}+\frac{e_x^2+e_y^2}{16}\right]\Big[(i_x^4-6i_x^2i_y^2+i_y^4)(e_xC_{\kappa+2\Theta}-e_yS_{\kappa+2\Theta})\\
&\qquad + 4(i_x^2-i_y^2)i_xi_y\big(e_xS_{\kappa+2\Theta}+e_yC_{\kappa+2\Theta}\big)+e_xC_{\kappa-2\Theta}-e_yS_{\kappa-2\Theta}\Big]\\
&+\left[1-\frac{5}{2}(e_x^2+e_y^2)+\frac{13}{16}(e_x^2+e_y^2)^2\right]\Big[(i_x^4-6i_x^2i_y^2+i_y^4)C_{2\kappa+2\Theta}+4(i_x^2-i_y^2)i_xi_yS_{2\kappa+2\Theta}\Big]\\
&+\left[\frac{7}{2}-\frac{123}{16}(e_x^2+e_y^2)\right]\Big[(i_x^4-6i_x^2i_y^2+i_y^4)(e_xC_{3\kappa+2\Theta}+e_yS_{3\kappa+2\Theta})\\
&\qquad + 4(i_x^2-i_y^2)i_xi_y\big(e_xS_{3\kappa+2\Theta}-e_yC_{3\kappa+2\Theta}\big)+e_xC_{3\kappa-2\Theta}-e_yS_{3\kappa-2\Theta}\Big]\\
&+\left[\frac{17}{2}-\frac{115}{6}(e_x^2+e_y^2)\right]\Big[(i_x^4-6i_x^2i_y^2+i_y^4)((e_x^2-e_y^2)C_{4\kappa+2\Theta}+2e_xe_yS_{4\kappa+2\Theta})\\
&\qquad + 4(i_x^2-i_y^2)i_xi_y\big((e_x^2-e_y^2)S_{4\kappa+2\Theta}-2e_xe_yC_{4\kappa+2\Theta}\big)+(e_x^2-e_y^2)C_{4\kappa-2\Theta}-2e_xe_yS_{4\kappa-2\Theta}\Big]\\
&+4\left[\frac{9}{4}+\frac{7}{4}(e_x^2+e_y^2)\right]\Big[\Big((i_x^2-i_y^2)C_{2\Theta}+2i_xi_yS_{2\Theta}\Big)\Big((e_x^2-e_y^2)C_{2\kappa}+2e_xe_yS_{2\kappa}\Big)\\
&+4\left[\frac{3}{2}+\frac{27}{16}(e_x^2+e_y^2)\right]\Big[\Big((i_x^2-i_y)^2C_{2\theta}+2i_xi_yS_{2\Theta}\Big)\Big(e_xC_K+e_yS_K\Big)\Big]\\
&+\frac{2}{(1-e_x^2-e_y^2)^{\frac{3}{2}}}\Big[(i_x^2-i_y^2)C_{2\Theta}+2i_xi_yS_{2\Theta}\Big]\Bigg\}
\end{aligned}
\tag{88}
$$

DOI: 10.13009/EUCASS2019-713

and:

$$
\begin{aligned}
V_{S_{22}}(x_{eoe}) = \frac{\mu R_e^2 S_{22}}{a^3}&\frac{3}{(1+i_x^2+i_y^2)^2}\Bigg\{\\
&\left[-\frac{1}{2}+\frac{e_x^2+e_y^2}{16}\right]\Big[-(i_x^4-6i_x^2i_y^2+i_y^4)(e_xS_{\kappa+2\Theta}+e_yC_{\kappa+2\Theta})\\
&\quad+4(i_x^2-i_y^2)i_xi_y\big(e_xC_{\kappa+2\Theta}-e_yS_{\kappa+2\Theta}\big)+e_xS_{\kappa-2\Theta}+e_yC_{\kappa-2\Theta}\Big]\\
&+\left[1-\frac{5}{2}(e_x^2+e_y^2)+\frac{13}{16}(e_x^2+e_y^2)^2\right]\Big[-(i_x^4-6i_x^2i_y^2+i_y^4)S_{2\kappa+2\Theta}+4(i_x^2-i_y^2)i_xi_yC_{2\kappa+2\Theta}\Big]\\
&+\left[\frac{7}{2}-\frac{123}{16}(e_x^2+e_y^2)\right]\Big[(i_x^4-6i_x^2i_y^2+i_y^4)(-e_xS_{3\kappa+2\Theta}+e_yC_{3\kappa+2\Theta})\\
&\quad+4(i_x^2-i_y^2)i_xi_y\big(e_xC_{3\kappa+2\Theta}+e_yS_{3\kappa+2\Theta}\big)+e_xS_{3\kappa-2\Theta}-e_yC_{3\kappa-2\Theta}\Big]\\
&+\left[\frac{17}{2}-\frac{115}{6}(e_x^2+e_y^2)\right]\Big[(i_x^4-6i_x^2i_y^2+i_y^4)(-(e_x^2-e_y^2)S_{4\kappa+2\Theta}+2e_xe_yC_{4\kappa+2\Theta})\\
&\quad+4(i_x^2-i_y^2)i_xi_y\big((e_x^2-e_y^2)C_{4\kappa+2\Theta}+2e_xe_yS_{4\kappa+2\Theta}\big)+(e_x^2-e_y^2)S_{4\kappa-2\Theta}-2e_xe_yC_{4\kappa-2\Theta}\Big]\\
&+4\left[\frac{9}{4}+\frac{7}{4}(e_x^2+e_y^2)\right]\Big[\big(2i_xi_yC_{2\theta}-(i_x^2-i_y)^2S_{2\Theta}\big)\big((e_x^2-e_y^2)C_{2\kappa}+2e_xe_yS_{2\kappa}\big)\\
&+4\left[\frac{3}{2}+\frac{27}{16}(e_x^2+e_y^2)\right]\Big[\big(2i_xi_yC_{2\theta}-(i_x^2-i_y)^2S_{2\Theta}\big)\big(e_xC_K+e_yS_K\big)\Big]\\
&+\frac{2}{(1-e_x^2-e_y^2)^{\frac{3}{2}}}\Big[2i_xi_yC_{2\theta}-(i_x^2-i_y)^2S_{2\Theta}\Big]\Bigg\}
\end{aligned}
\tag{89}
$$

with C_{22} and S_{22} the Earth gravitational potential Legendre coefficients of degree 2 and order 2. Their values are given in Appendix C.

B. Linearized Linear Time Varying GEO Dynamics

The matrices of the linearized dynamics (5) are given by:

$$A(t) = A_K + A_{C_{20}}(t) + A_{C_{21}}(t) + A_{S_{21}}(t) + A_{C_{22}}(t) + A_{S_{22}}(t), \tag{90a}$$

$$D(t) = D_K + D_{C_{20}}(t) + D_{C_{21}}(t) + D_{S_{21}}(t) + D_{C_{22}}(t) + D_{S_{22}}(t), \tag{90b}$$

$$A_K = \gamma_K \begin{bmatrix} 0 & 0 & 0 & 0 & 0 & 0 \\ 0 & 0 & 0 & 0 & 0 & 0 \\ 0 & 0 & 0 & 0 & 0 & 0 \\ 0 & 0 & 0 & 0 & 0 & 0 \\ 0 & 0 & 0 & 0 & 0 & 0 \\ 1 & 0 & 0 & 0 & 0 & 0 \end{bmatrix}, \tag{91a}$$

$$D_K = \delta_K \begin{bmatrix} 0 & 0 & 0 & 0 & 0 & 1 \end{bmatrix}^T, \tag{91b}$$

$$\gamma_K = -\frac{3}{2}\sqrt{\frac{\mu}{a_{sk}^3}}, \qquad \delta_K = \sqrt{\frac{\mu}{a_{sk}^3}} - \omega_e, \tag{91c}$$

DOI: 10.13009/EUCASS2019-713

$$A_{C_{20}} = \alpha_{20} \begin{bmatrix} 0 & S_\kappa & C_\kappa & 0 & 0 & 0 \\ \frac{7}{4}S_\kappa & -\frac{3}{2}S_{2\kappa} & -\frac{1}{2}(1-3C_{2\kappa}) & 0 & 0 & -\frac{1}{2}C_\kappa \\ -\frac{7}{4}C_\kappa & \frac{1}{2}(1+3C_{2\kappa}) & \frac{3}{2}S_{2\kappa} & 0 & 0 & -\frac{1}{2}S_\kappa \\ 0 & 0 & 0 & -\frac{1}{2}S_{2\kappa} & \frac{1}{2}(1+C_{2\kappa}) & 0 \\ 0 & 0 & 0 & \frac{1}{2}(C_{2\kappa}-1) & \frac{1}{2}S_{2\kappa} & 0 \\ \frac{7}{2} & -\frac{13}{4}C_\kappa & -\frac{13}{4}S_\kappa & 0 & 0 & 0 \end{bmatrix}, \tag{92a}$$

$$D_{C_{20}} = \alpha_{21} \begin{bmatrix} 0 & -\frac{1}{2}S_\kappa & \frac{1}{2}C_\kappa & 0 & 0 & -1 \end{bmatrix}^T, \tag{92b}$$

$$\alpha_{20} = \sqrt{\frac{\mu}{a_{sk}}} \frac{3R_e^2 C_{20}}{a_{sk}^3} \tag{92c}$$

$$A_{C_{21}} = \alpha_{21} \begin{bmatrix} 0 & 0 & 0 & 4(C_\kappa C_\ell - S_\kappa S_\ell) & 4(S_\kappa C_\ell + C_\kappa S_\ell) & 0 \\ 0 & 0 & 0 & 6S_\kappa^2 C_\ell & -6C_\kappa S_\kappa C_\ell & 0 \\ 0 & 0 & 0 & -6C_\kappa S_\kappa C_\ell & 6C_\kappa^2 C_\ell & 0 \\ \frac{7}{4}C_\kappa C_\ell & -\frac{3}{2}C_\kappa^2 C_\ell & -\frac{3}{2}C_\kappa S_\kappa C_\ell & 0 & 0 & \frac{1}{2}(S_\kappa C_\ell + C_\kappa S_\ell) \\ \frac{7}{4}S_\kappa C_\ell & -\frac{3}{2}C_\kappa S_\kappa C_\ell & -\frac{3}{2}S_\kappa^2 C_\ell & 0 & 0 & \frac{1}{2}(S_\kappa S_\ell - C_\kappa C_\ell) \\ 0 & 0 & 0 & 11S_\kappa C_\ell & -1C_\kappa C_\ell & 0 \end{bmatrix}, \tag{93a}$$

$$D_{C_{21}} = \alpha_{21} \begin{bmatrix} 0 & 0 & 0 & \frac{1}{2}C_\kappa C_\ell & \frac{1}{2}S_\kappa C_\ell & 0 \end{bmatrix}^T, \tag{93b}$$

$$\alpha_{21} = \sqrt{\frac{\mu}{a_{sk}}} \frac{3R_e^2 C_{21}}{a_{sk}^3} \tag{93c}$$

$$A_{S_{21}} = \beta_{21} \begin{bmatrix} 0 & 0 & 0 & 4(S_\kappa C_\ell + C_\kappa S_\ell) & 4(S_\kappa S_\ell - C_\kappa C_\ell) & 0 \\ 0 & 0 & 0 & 6S_\kappa^2 S_\ell & -6C_\kappa S_\kappa S_\ell & 0 \\ 0 & 0 & 0 & -6C_\kappa S_\kappa S_\ell & 6C_\kappa^2 S_\ell & 0 \\ \frac{7}{4}C_\kappa S_\ell & -\frac{3}{2}C_\kappa^2 S_\ell & -\frac{3}{2}C_\kappa S_\kappa S_\ell & 0 & 0 & -\frac{1}{2}(S_\kappa C_\ell + C_\kappa S_\ell) \\ \frac{7}{4}S_\kappa C_\ell & -\frac{3}{2}C_\kappa S_\kappa C_\ell & -\frac{3}{2}S_\kappa^2 C_\ell & 0 & 0 & \frac{1}{2}(C_\kappa C_\ell - S_\kappa S_\ell) \\ 0 & 0 & 0 & -11S_\kappa S_\ell & 11C_\kappa S_\ell & 0 \end{bmatrix}, \tag{94a}$$

$$D_{S_{21}} = \beta_{21} \begin{bmatrix} 0 & 0 & 0 & -\frac{1}{2}C_\kappa S_\ell & -\frac{1}{2}S_\kappa S_\ell & 0 \end{bmatrix}^T, \tag{94b}$$

$$\beta_{21} = \sqrt{\frac{\mu}{a_{sk}}} \frac{3R_e^2 C_{21}}{a_{sk}^3} \tag{94c}$$

$$A_{C_{22}} = \alpha_{22} \begin{bmatrix} 10S_{2\ell} & S_{\kappa 2\Theta} - 21S_{3\kappa 2\Theta} & C_{\kappa 2\Theta} + 21C_{3\kappa 2\Theta} & 0 & 0 & -8C_{2\ell} \\ -\frac{7}{4}(S_{\kappa 2\Theta} + 7S_{3\kappa 2\Theta}) & 17S_{4\kappa 2\Theta} - S_{2\ell} & -5C_{2\ell} - 17C_{4\kappa 2\Theta} & 0 & 0 & \frac{1}{2}(C_{\kappa 2\Theta} + 21C_{3\kappa 2\Theta}) \\ -\frac{7}{4}(C_{\kappa 2\Theta} - 7C_{3\kappa 2\Theta}) & 5C_{2\ell} - 17C_{4\kappa 2\Theta} & -17S_{4\kappa 2\Theta} - S_{2\ell} & 0 & 0 & \frac{1}{2}(-S_{\kappa 2\Theta} + 21S_{3\kappa 2\Theta}) \\ 0 & 0 & 0 & -S_{2\ell} + S_{2\Theta} & -C_{2\ell} - C_{2\Theta} & 0 \\ 0 & 0 & 0 & C_{2\ell} - C_{2\Theta} & -S_{2\ell} - S_{2\Theta} & 0 \\ -21C_{2\ell} & \frac{11}{4}(-C_{\kappa 2\Theta} + 7C_{3\kappa 2\Theta}) & \frac{11}{4}(S_{\kappa 2\Theta} + 7S_{3\kappa 2\Theta}) & 0 & 0 & -12S_{2\ell} \end{bmatrix}, \tag{95a}$$

$$D_{C_{22}} = \alpha_{22} \begin{bmatrix} -4S_{2\ell} & \dfrac{1}{2}(S_{\kappa 2\Theta} + 7S_{3\kappa 2\Theta}) & \dfrac{1}{2}(C_{\kappa 2\Theta} - 7C_{3\kappa 2\Theta}) & 0 & 0 & 6C_{2\ell} \end{bmatrix}, \tag{95b}$$

$$\alpha_{22} = \sqrt{\frac{\mu}{a_{sk}}} \frac{3R_e^2 C_{21}}{a_{sk}^3} \tag{95c}$$

with:

$$\begin{cases} C_{2\Theta} = \cos(2\Theta), \\ S_{2\Theta} = \sin(2\Theta), \end{cases} \quad \begin{cases} C_{\kappa 2\Theta} = \cos(\kappa_{sk} - 2\Theta), \\ S_{\kappa 2\Theta} = \sin(\kappa_{sk} - 2\Theta), \end{cases}$$
$$\begin{cases} C_{3\kappa 2\Theta} = \cos(3\kappa_{sk} - 2\Theta), \\ S_{3\kappa 2\Theta} = \sin(3\kappa_{sk} - 2\Theta), \end{cases} \quad \begin{cases} C_{4\kappa 2\Theta} = \cos(4\kappa_{sk} - 2\Theta), \\ S_{4\kappa 2\Theta} = \sin(4\kappa_{sk} - 2\Theta). \end{cases} \tag{96}$$

DOI: 10.13009/EUCASS2019-713

$$A_{S_{22}} = \beta_{22} \begin{bmatrix} -10C_{2\ell} & -C_{\kappa 2\Theta} + 21C_{3\kappa 2\Theta} & S_{\kappa 2\Theta} + 21S_{3\kappa 2\Theta} & 0 & 0 & -8S_{2\ell} \\ \frac{7}{4}(C_{\kappa 2\Theta} + 7C_{3\kappa 2\Theta}) & -17C_{4\kappa 2\Theta} + C_{2\ell} & -5S_{2\ell} - 17S_{4\kappa 2\Theta} & 0 & 0 & \frac{1}{2}(S_{\kappa 2\Theta} + 21S_{3\kappa 2\Theta}) \\ -\frac{7}{4}(S_{\kappa 2\Theta} - 7S_{3\kappa 2\Theta}) & 5S_{2\ell} - 17S_{4\kappa 2\Theta} & 17C_{4\kappa 2\Theta} + C_{2\ell} & 0 & 0 & \frac{1}{2}(C_{\kappa 2\Theta} - 21C_{3\kappa 2\Theta}) \\ 0 & 0 & 0 & C_{2\ell} + C_{2\Theta} & -S_{2\ell} + S_{2\Theta} & 0 \\ 0 & 0 & 0 & S_{2\ell} + S_{2\Theta} & C_{2\ell} - C_{2\Theta} & 0 \\ -21S_{2\ell} & -\frac{11}{4}(S_{\kappa 2\Theta} + 7S_{3\kappa 2\Theta}) & -\frac{11}{4}(C_{\kappa 2\Theta} + 7C_{3\kappa 2\Theta}) & 0 & 0 & 12C_{2\ell} \end{bmatrix}, \tag{97a}$$

$$D_{S_{22}} = \beta_{22} \begin{bmatrix} 4C_{2\ell} \\ -\frac{1}{2}(C_{\kappa 2\Theta} + 7C_{3\kappa 2\Theta}) \\ \frac{1}{2}(S_{\kappa 2\Theta} - 7S_{3\kappa 2\Theta}) \\ 0 \\ 0 \\ 6S_{2\ell} \end{bmatrix}, \tag{97b}$$

$$\beta_{22} = \sqrt{\frac{\mu}{a_{sk}}} \frac{3R_e^2 C_{21}}{a_{sk}^3} \tag{97c}$$

$$B(t) = \begin{bmatrix} 0 & 2 & 0 \\ S_\kappa & 2C_\kappa & 0 \\ -C_\kappa & 2S_K & 0 \\ 0 & 0 & \frac{1}{2}C_\kappa \\ 0 & 0 & \frac{1}{2}S_\kappa \\ -2 & 0 & 0 \end{bmatrix}, \tag{98}$$

$$C(t) = \begin{bmatrix} a_{sk} & -a_{sk}C_\kappa & -a_{sk} & 0 & 0 & 0 \\ 0 & 0 & 0 & 2S_\kappa & -2C_\kappa & 0 \\ 0 & 2S_\kappa & -2C_\kappa & 0 & 0 & 1 \end{bmatrix}. \tag{99}$$

C. Physical Parameters

This appendix gives numerical values for the physical parameters involved in the proposed article. In the sequel, the unit d stands for "day".

The physical and orbital parameters of the Earth are:

- geocentric gravitational parameter: $\mu = 3.986\ 10^5 \text{km}^3/\text{s}^2 = 2.9755\ 10^{15} \text{km}^3/\text{d}^2$,
- mean rotation rate: $\omega_e = 7.2921\ 10^{-5}\text{rad/s} = 6.3004\text{rad/d}$,
- coefficient of the spherical decomposition of the Earth gravitational field: see the Table **??** (these values have been taken from the reference Vallado[33]),
- sidereal angle $\Theta(t)$: using the computation algorithm from Vallado,[33] for January 1st, 2034, the value of the sidereal angle is: $\Theta_0 = 1.7579$ rad. If t denotes the elapsed time since January 1st, 2034, the sidereal angle at time t is computed as: $\Theta(t) = \Theta_0 + \omega_e t$ (for dates before the reference date, t has to be counted negatively),
- geostationary semi-major axis: $a_{sk} = 42165.8$km.

References

[1] P. J. Antsaklis. *Linear Systems*. Cambridge Aerospace Series. Birkhäuser, Boston, Massachusetts, USA, 2003.

[2] B. M. Anzel. Controlling a stationary orbit using electric propulsion. In *DGLR/AIAA/JSASS 20th International Electric propulsion Conference*, pages 306–314, Garmisch-Partenkirchen, Germany, 1988.

DOI: 10.13009/EUCASS2019-713

degree l	order m	C_{lm}	S_{lm}
2	0	$-1.083\ 10^{-3}$	$\times$
2	1	$-2.414\ 10^{-10}$	$1.543\ 10^{-9}$
2	2	$1.574\ 10^{-6}$	$-9.038\ 10^{-7}$

Table 1: C_{lm} and S_{lm} coefficients for the spherical harmonics decomposition of the Earth gravitational potential (values taken from Vallado[33]). The $\times$ means that for order 0, the S_{l0} coefficient does not exist.

[3] C. C. Barrett. On the Application of electric Propulsion to Satellite Orbit Adjustement and Station Keeping. In *American Institute of Aeronautics and Astronautics, Electric propulsion and Plasmadynamics Conference*, Colorado Springs, Colorado, 1967.

[4] Richard H. Battin. *An Introduction to the Mathematics and Methods of Astrodynamics*. Education. AIAA., 1999.

[5] J. T. Betts. Survey of Numerical Methods for Trajectory Optimization. *Journal of Guidance, Control, and Dynamics*, 21(2):193–207, 1998.

[6] M. Brentari, S. Urbina, D. Arzelier, C. Louembet, and L. Zaccarian. A hybrid control framework for impulsive control of satellite rendezvous. *IEEE Transactions on Control Systems Technology*, (99):1–15, 2018.

[7] G. Deaconu, C. Louembet, and A. Théron. Constrained periodic spacecraft relative motion using non-negative polynomials. In *2012 American Control Conference (ACC)*, pages 6715–6720. IEEE, 2012.

[8] A. Demairé and H. Gray. Plasma propulsion system functional chain first three years in orbit on eurostar 3000. In *30th International Electric Propulsion Conference, IEPC-2007-060*, 2007.

[9] S. S. Farahani, I. Papusha, Ca. McGhan, and R. M. Murray. Constrained autonomous satellite docking via differential flatness and model predictive control. In *2016 IEEE 55th Conference on Decision and Control (CDC)*, pages 3306–3311. IEEE, 2016.

[10] M. Fliess, J. Lévine, P. Martin, and P. Rouchon. On differentially flat nonlinear systems. In *Nonlinear Control Systems Design*, pages 159–163. Elsevier, 1993.

[11] M. Fliess, J. Lévine, P. Martin, and P. Rouchon. A lie-bäcklund approach to equivalence and flatness of nonlinear systems. *IEEE Transactions on Automatic Control*, 44(5):922–937, 1999.

[12] M. Fliess, P. Martin, and P. Rouchon. Differential flatness and defect : an overview. *Geometry in Nonlinear Control and Differential Inclusions*, 32:209–225, 1995.

[13] Michel Fliess, Jean Lévine, Philippe Martin, and Pierre Rouchon. International Journal of Control. *International Journal of Control*, 61(6):1327–1361, 1995.

[14] H. Ford, L. R. Hunt, and R. Su. A simple algorithm for computing canonical forms. *Computers & Mathematics with Applications*, 10(4):315–326, 1984.

[15] C. R. Hargraves and S. W. Paris. Direct Trajectory Optimization Using Nonlinear Programming and Collocation.pdf. *Journal of Guidance, Control, and Dynamics*, 10(4):338–342, 1987.

[16] D. G. Hull. Conversion of Optimal Control Problems into Parameter Optimization Problems. *Journal of Guidance, Control, and Dynamics*, 20(1):57–60, 1997.

[17] R. R. Hunziker. Low-Thrust Station Keeping Guidance for a 24-Hour Satellite. *AIAA Journal*, 8(7):1186–1192, 1970.

[18] E. T. Y. Lee. A simplified b-spline computation routine. *Computing*, 29(4):365–371, Dec 1982.

[19] J. Lévine. On necessary and sufficient conditions for differential flatness. *Applicable Algebra in Engineering, Communications and Computing*, 22(1):47–90, 2011.

[20] Jean Lévine and D. V. Nguyen. Flat output characterization for linear systems using polynomial matrices. *systems & Control Letters*, 48:69–75, 2003.

DOI: 10.13009/EUCASS2019-713

[21] D. Losa. *High vs low thrust station keeping maneuver planning for geostationary satellites*. PhD thesis, Ecole Nationale des Mines de Paris, 2007.

[22] C. Louembet, F. Cazaurang, A. Zolghadri, C. Charbonnel, and C. Pittet. Path planning for satellite slew manoeuvres: a combined flatness and collocation-based approach. *IET control theory & applications*, 3(4):481–491, 2009.

[23] Christophe Louembet and Georgia Deaconu. Collision avoidance in low thrust rendezvous guidance using flatness and positive b-splines. In *Proceedings of the 2011 American Control Conference*, pages 456–461. IEEE, 2011.

[24] P. Martin, P. Rouchon, and R. M. Murray. Flat Systems, Equivalence and Trajectory Generation. *CDS Technical Report*, pages 1–79, 2003.

[25] M. Milam, K. Mushambi, and R. Murray. A new computational approach to real-time trajectory generation for constrained mechanical systems. In *Decision and Control, 2000. Proceedings of the 39th IEEE Conference on*, volume 1, pages 845–851. IEEE, 2000.

[26] R. M. Murray, M. Rathinam, and W. Sluis. Differential flatness of mechanical control systems: A catalog of prototype systems. In *ASME international mechanical engineering congress and exposition*. Citeseer, 1995.

[27] T. Neckel, C. Talbot, and N. Petit. Collocation and inversion for a reentry optimal control problem. In *5th International Conference on Launcher Technology*, 2003.

[28] H.H. Rosenbrock. *State-space and multivariable theory*. Nelson, 1970.

[29] R. E. Sherrill, A. J. Sinclair, S.C. Sinha, and T. A. Lovell. Lyapunov-floquet control of satellite relative motion in elliptic orbits. *IEEE Transactions on Aerospace and Electronic Systems*, 51(4):2800–2810, 2015.

[30] Marcel J. Sidi. *Spacecraft Dynamics and Control*. Cambridge University Press, 1997.

[31] E. D. Sontag. *Sontag, E. D. Mathematical control theory: deterministic finite dimensional systems*. Springer Science & Business Media, 2013.

[32] E. M. Soop. *Handbook of Geostationary Orbits*. Kluwer Academic Publishers Group, 1994.

[33] David A. Vallado. *Fundamentals of Astrodynamics and Applications*. Space Technology Series, 1997.